Direct View of Structural Regimes of End-Grafted Polymer Monolayers: A Scanning Force Microscopy Study

V. Koutsos, E. W. van der Vegte, and G. Hadziioannou*

Department of Polymer Chemistry, University of Groningen, Nijenborgh 4, 9747 AG Groningen, The Netherlands

Received November 18, 1997; Revised Manuscript Received July 17, 1998

ABSTRACT: Scanning force microscopy images of thiol-end-functionalized polystyrene monolayers, end-grafted to gold substrates from good solvent, showed two structural regimes in bad-solvent conditions. At low and moderate grafting densities the experimental results agree with the scaling arguments and can be situated correctly to the corresponding diagram of states for single end-grafted chains and pinned micelles, respectively. A third structural regime, of semicontinuous dimples, has been observed when adsorption was performed from poor-solvent conditions.

Introduction

End-grafted polymer monolayers play an important role in colloidal stabilization,[1,2] adhesion,[3] and biocompatibility of artificial organs in medicine.[4] In good-solvent conditions the physical picture is rather simple. In connection with grafting density, two limiting regimes can be distinguished:[5] at low grafting densities, each chain is isolated, occupying roughly a half-sphere with a radius comparable to the radius of gyration ("mushroom" regime); at high grafting densities, polymers stretch away from the interface to avoid overlapping, forming a uniform polymer "brush".

In bad-solvent conditions (dry state) the structural forms have a wider variety. When the grafting density is low enough, the polymer chains collapse separately.[6] If the polymer chains overlap with each other, they collapse in groups due to the polymer−polymer attractive interactions and the constraints of the grafted tethers, forming clusters. This microphase segregation has been detected by several scanning force microscopy studies[6,7] in agreement with theoretical and numerical predictions.[8] For even higher grafting densities the situation becomes trivial: a homogeneous layer can be formed.[7b]

Recently, much work has been focused on the structural states of the end-grafted monolayers in bad-solvent conditions. In a previous study of ours[6] we used the spontaneous chemisorption of thiol-terminated polystyrene (PS−SH) on gold surfaces from toluene solutions to form monolayers of end-grafted PS. We described the single chains−cluster transition and showed that the cluster dimensions agree with scaling predictions for pinned micelles.[8g,h]

In this paper (a) we present some more data on the single chain regime and demonstrate that our previous and recent data fit well in a diagram of states deduced by scaling arguments and (b) we show that, for high grafting densities and before a homogeneous layer is formed, there is an intermediate regime of semicontinuous dimples.

Experimental Part

Gold Substrate Preparation. Mica was cleaved in air and immediately placed in the vacuum chamber of a diffusion pump thermal evaporator (Edwards Auto 306). The mica sheets were heated to 400 °C at a pressure below 1×10^{-4} mbar. Gold was evaporated from resistively heated tungsten boats at a pressure below 5×10^{-6} mbar. The thickness of the gold layer was monitored with a quartz crystal oscillator and eventually amounted to 35 nm (deposition rate 3 nm/min). The gold substrates were left at 400 °C for 2 h and then cooled to room temperature in a vacuum. The vacuum chamber was filled with prepurified nitrogen, and the gold substrates were removed and stored under nitrogen until further use. This way of gold film preparation produces atomically flat gold islands separated by deep channels.[9,10]

Table 1. Molecular Characteristics of the PS_x-SH[α] Polymers and Grafting Densities Estimated from SFM Images

polymer	M_w	M_w/M_n	σ (no. of chains/μm^2)
PS_{400}−SH	41 500	1.09	22 839
PS_{500}−SH	51 500	1.1	19 929
PS_{800}−SH	85 000	1.2	14 688
PS_{1400}−SH	144 000	1.2	12 672
PS_{2500}−SH	258 000	1.1	4 268
PS_{1400}−SH (lower coverage)	144 000	1.2	3 800

[α] The subscript refers to the approximate degree of polymerization.

Sample Preparation. Thiol-terminated polystyrene (PS−SH) was prepared by anionic polymerization.[11,12] For the first topic of this study the samples were prepared by exposing the gold substrates to a 0.1 mg/mL toluene (good solvent for PS) solution of PS_{1400}−SH (molecular weight 144 000, polydispersity 1.2) for relatively short incubation time (so that low grafting density is attained[6]). In addition, a group of data from our paper, ref 6, was used. The gold substrates were immersed in 2 mg/mL solutions of PS_x−SH (five different molecular weights) for 48 h (Table 1). For one molecular weight (PS_{1400}−SH), we also employed a 0.1 mg/mL solution and 24 h of incubation time. Using long incubation times, we obtained higher surface coverages.[6] For all samples, the substrates were removed from the adsorption solution and immediately rinsed exhaustively with fresh toluene. The samples were dried under a stream of argon and were placed in a vacuum at 50 °C for 1 h and stored in nitrogen.

For the second topic (higher grafting densities−dimples formation) we used a 0.1 mg/mL cyclohexane (poor solvent for PS at room temperature) solution of PS_{1400}−SH. The gold substrates were kept in the solution for 1 h. Immediately after their removal from the cyclohexane solution and the rinsing with fresh toluene, they were dipped in pure toluene for about 1 h. This step is important since we want to exclude the possibility of physisorbed polymer chains on the substrate.

* To whom correspondence should be addressed. E-mail Hadzii@chem.rug.nl.

10.1021/ma971702k CCC: $18.00
Published on Web 02/02/1999

Scanning Force Microscopy. All scanning force microscopy[13] experiments have been performed in water (bad solvent for PS−SH molecules) using a Topometrix SFM (Explorer). We imaged the samples in contact mode (tip in contact with the surface), keeping the applied force constant. Commercially available Si_3N_4, V-shaped cantilevers (spring constant 0.032 N/m) were used. The imaging was performed in water in order to eliminate any meniscus forces and at an applied force approximately equal to the adhesive force to avoid distortion of the polymer layer (as described in our paper, ref 6). Several samples were made for each incubation time, and each sample was imaged at different areas. Similar pictures were obtained, demonstrating the reproducibility of the results. All images are shown without any image processing except horizontal leveling.

Theoretical Background

Using scaling arguments, Zhulina et al.[8h] constructed a diagram of states for the case of a system of polymer chains end-grafted to a planar surface. Depending on the degree of polymerization, the solvent quality, and the grafting density, several structural regimes were predicted. Here, we give a brief description of the physics involved for the particular case of bad-solvent conditions.

We consider a system of polymer chains (degree of polymerization N) end-grafted onto a planar surface. We have chosen the chain unit α as the unit length (all dimensions are expressed in α units). Since we investigated the polymer morphology exclusively in the case of bad-solvent conditions where the solvent is completely expelled from the polymer, we have taken the relative deviation from the θ-point ($\tau = (\theta - T)/\theta$) as constant and equal to 1. Hence, the second virial coefficient is $v = -\tau\alpha^3 = -\alpha^3 < 0$.

In the case of isolated polymer chains, the polymer chains collapse separately, forming individual single-chain globules of radius $R_s \cong N^{1/3}$ and free energy (the volume free energy has been taken as the reference state)

$$F_s/kT \cong R_s^2 \cong N^{2/3} \tag{1}$$

At moderate grafting densities σ the polymer chains fuse to form pinned micelles[8g−i] due to the competition between the attractive forces and the grafting constraints. The free energy per chain scales as[8h]

$$F_m/kT \cong N^{2/5}\sigma^{-1/5} \tag{2}$$

At higher grafting densities σ, we expect that the microsegregation tendency decreases, and ultimately a homogeneous brush forms. The free energy per chain of the homogeneous layer is

$$F_b/kT \cong \sigma^{-1} \tag{3}$$

Comparing the free energies per chain in a micelle (2) and in other possible structures—separate single chains (1) and homogeneous grafted layer (3)—one finds that such micelles are stable when

$$N^{-4/3} = \sigma_I < \sigma < \sigma_{II} = N^{-1/2} \tag{4}$$

At $\sigma \ll \sigma_I$, the chains form individual single-chain globules whereas at $\sigma \gg \sigma_{II}$ the pinned micelles coalesce into a homogeneous, collapsed grafted layer.

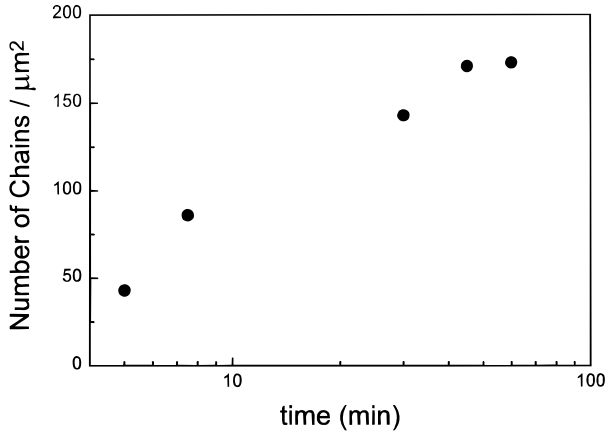

Figure 1. Time evolution for the chemisorption process of PS_{1400}−SH onto the gold surface from 0.1 mg/mL toluene solution.

Results and Discussion

Diagram of States. We immersed gold substrates in a toluene solution of PS_{1400}−SH for different relatively short incubation times. On flat gold terraces, well-separated collapsed single chains could be seen.[6] For each incubation time, the grafting density (number of end-grafted chains per μm^2) was measured directly by counting the number of single-chain globules from SFM images. In Figure 1 we present time-dependent adsorption data. The grafting polymer density increases with the incubation time.

In Figure 2a we have situated our data in a diagram of states defined by relation 4. The different regimes are presented in $x = (\sigma N)^{-1}$ and $y = N^{1/2}$ variables. The squares correspond to the samples prepared within short adsorption times. (This is the same group of data used also for the construction of the isotherm in Figure 1.) The circles correspond to samples prepared within long adsorption times. (This group of data involves PS−SH polymers with different molecular weights and is taken from our paper, ref 6.) In ref 6, we estimated the polymer mass coverages from topographical SFM images. The grafting densities (for long adsorption times) were calculated directly using these mass coverages. In the last column of Table 1, we show the estimated grafting densities for each PS_x−SH polymer (the subscript refers to the approximate degree of polymerization). For both cases the PS Kuhn length (α = 0.55 nm, we assume that the Kuhn segment is of the order of the chain unit α) has been taken as the unit length. The experimental points verify the regimes predicted by the scaling arguments. An increase in grafting density σ for a specific molecular weight (fixed $N = 1385$) corresponds to the intersection of the diagram along the dashed line. In agreement with the experimental data, as the grafting density increases, one passes from the single-chain globule regime to the pinned-micelle regime.

Figure 2b is a magnification of the diagram of Figure 2a close to the origin of the axes (dotted rectangle). Two SFM images for the pinned micelles and one for the single-chain globules are shown. We observe well-defined polymer clusters adsorbed on flat gold islands separated by steep channels. The topographical features of these monolayers depend both on polymer molecular weight and on the grafting density (for details see ref

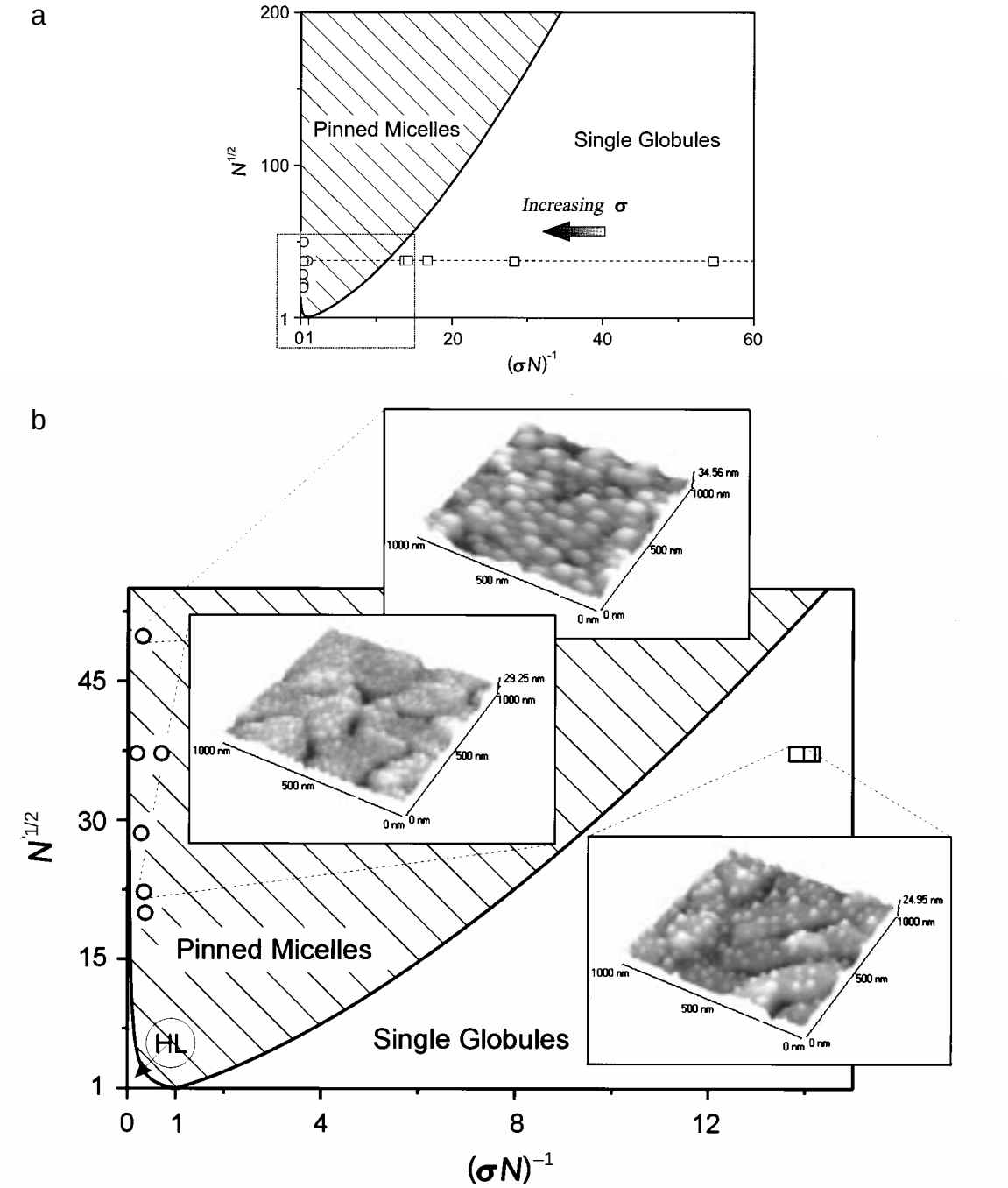

Figure 2. (a, top) Diagram of states of grafted polymer layers. The pinned-micelle regime occupies a substantial area of the diagram.The measurements on samples immersed in the solution for short incubation times correspond to points well within the single globule regime. (b, bottom) Magnification of the diagram of states near the origin of the axes. All three regimes can be seen. For very high grafting densities the grafted layer becomes homogeneous (HL). The measurements on substrates immersed into toluene solutions for long adsorption times are in the pinned-micelle regime.

6). It is clear that the experimental points for the pinned micelles are well in the corresponding regime although not far away from the homogeneous-layer regime. The transitions between the regimes are expected to be gradual since nonuniform grafting densities and statistical fluctuations could lead to irregular spatial distributions of clusters.

Adsorption from Poor Solvents—Formation of Dimples. In Figure 3a,b we present a SFM topography image and a line scan, respectively, for the surface of grafted PS_{1400}—SH on the gold substrate from a cyclohexane (poor solvent for PS at room temperature) solution. The imaging has been performed under water (bad solvent for PS). Although the microphase separation is still evident, in contrast to the previous images of the monolayers that were prepared in good-solvent conditions and were organized in well-separated clusters, the polymer monolayer prepared from poor-solvent conditions is organized in semicontinuous dimples. The reason for the phase separation in the microscale is the same as for the formation of the pinned micelles: competition between the attractive polymer—polymer interactions and the permanent grafting constraints. However, the structural transition from individual clusters (pinned micelles) to dimples is a result of the different solvent conditions during the brush formation. It is well-known that synthesis of grafted polymer brushes in poor-solvent conditions results in high graft-

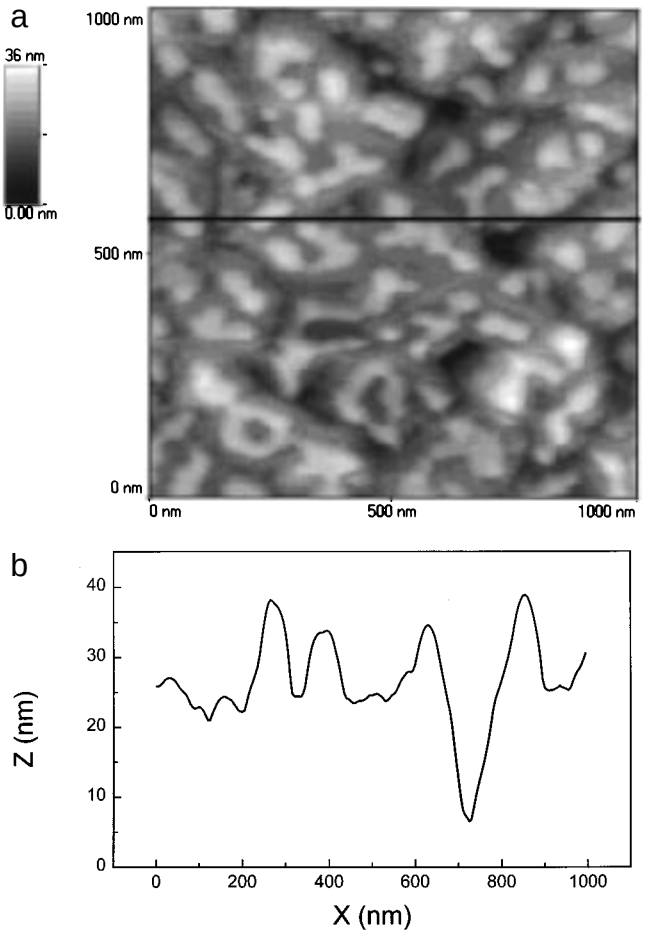

Figure 3. (a, top) Topography of a collapsed PS_{1400}−SH brush that has been formed in poor-solvent conditions (concentration 0.1 mg/mL, incubation time 1 h). (b, bottom) Height profile along a typical line scan (black line in (a)). We observe a cross-sectional view of the dimples formed on a flat gold island. A steep gold channel can be clearly seen on the right.

ing densities since the attractive polymer−polymer interactions largely nullify the repulsive steric interactions. This higher grafting density results in a less effective phase separation with the formation of a quite regular dimpled surface. This pattern is consistent with simulations[8d,e] and calculations[8b] in the case of relatively high and uniform grafting density. The width and height of the dimples are about 80 and 12 nm, respectively. Since the radius of gyration of a collapsed PS_{1400}−SH chain is $R_c = aN^{1/3} \approx 6.1$ nm, the dimple formation involves several chains. The average distance between the dimples is about 120 nm. Yeung et al.[8b] predicted that the mean spacing between the dimples (for a system close to the θ-temperature) is on the order of the radius of gyration for a polymer chain in a Θ-solvent. In addition, Soga et al.[8e] using Monte Carlo simulations found that this distance is independent of solvent quality. Contrary to these predictions, our results suggest that the average distance between the dimples is 6 times the radius of gyration for a PS_{1400}−SH chain in a Θ-solvent ($R_\Theta = aN^{1/2} \approx 20$ nm). This discrepancy could arise from the abrupt change in solvent quality in our experiments.

In view of the diagram of states described above, the dimple morphology could correspond to another regime, intermediate between the pinned-micelle and the homogeneous-layer regime, which simple scaling analysis fails to capture.

Conclusions

The spontaneous chemisorption of PS−SH molecules on Au surfaces from a solution in good solvent results in two structural regimes as observed, with AFM, in bad solvent. These are the single collapsed chain and pinned micelles fitting in the diagram of states as predicted by scaling arguments. The chemisorption of PS−SH molecules to gold from poor-solvent conditions produced a qualitatively different result where the polymer monolayer organizes itself in the form of semicontinuous dimples, constituting an additional regime in the diagram of states.

Acknowledgment. We thank Amalia Stamouli for her careful reading of the manuscript. This work was financially supported by The Netherlands Foundation for Fundamental Research on Matter (FOM).

References and Notes

(1) Napper, D. *Polymeric Stabilization of Colloidal Dispersions*; Academic Press: London, 1983.
(2) Gast, A.; Leibler, L. *Macromolecules* **1986**, *19*, 686.
(3) Lee, L. H. *Adhesion and Adsorption of Polymers*; Plenum Press: New York, 1980.
(4) Ruckenstein, E.; Chang, D. B. J. *Colloid Interface Sci.* **1988**, *123*, 170.
(5) De Gennes, P. G. *Macromolecules* **1980**, *13*, 1069.
(6) Koutsos, V.; van der Vegte, E. W.; Pelletier, E.; Stamouli, A.; Hadziioannou, G. *Macromolecules* **1997**, *30*, 4719.
(7) (a) Zhao, W.; Krausch, G.; Rafailovich, M. H.; Sokolov, J. *Macromolecules* **1994**, *27*, 2933. (b) Siqueira, D. F.; Köhler, K.; Stamm, M. *Langmuir* **1995**, *11*, 3092. (c) Karim, A.; Tsukruk, V. V.; Douglas, J. F.; Satija, S. K.; Fetters, L. J.; Reneker, D. H.; Foster, M. D. *J. Phys. II* **1995**, *5*, 1441. (d) Stamouli, A.; Pelletier, E.; Koutsos, V.; van der Vegte, E. W.; Hadziioannou, G. *Langmuir* **1996**, *12*, 3221. (e) Spatz, J. P.; Sheiko, S.; Möller, M. *Adv. Mater.* **1996**, *8*, 513.
(8) (a) Ross, R. S.; Pincus, P. *Europhys. Lett.* **1992**, *19*, 79. (b) Yeung, C.; Balazs A. C.; Jasnow, D. *Macromolecules* **1993**, *26*, 1914. (c) Tang, H.; Szleifer, I. *Europhys. Lett.* **1994**, *28*, 19. (d) Lai, P.-Y.; Binder, K. J. *J. Chem. Phys.* **1992**, *97*, 586. (e) Soga K. G.; Guo, H.; Zuckermann, M. J. *Europhys. Lett.* **1995**, *29*, 531. (f) Grest, G. S.; Murat, M. *Macromolecules* **1993**, *26*, 3108. (g) Williams, D. R. M. *J. Phys. II* **1993**, *3*, 1313. (h) Zhulina, E. B.; Birshtein, T. M.; Priamitsyn, V. A.; Klushin, L. I. *Macromolecules* **1995**, *28*, 8612. (i) Klushin, L. I., unpublished results.
(9) Zheng, X.-Y.; Ding, Y.; Bottomley, L. A. *J. Vac. Sci. Technol. B* **1995**, *13*, 1320.
(10) Koutsos, V.; van der Vegte, E. W.; Grim, P. C. M.; Hadziioannou, G. *Macromolecules* **1998**, *31*, 116.
(11) Stouffer, J. M.; McCarthy, T. J. *Macromolecules* **1988**, *21*, 1204.
(12) Tang, W. T. Study of block copolymer micelles in dilute solution by light scattering and fluorescence spectroscopy. Dissertation, Stanford University, 1987; pp 28−33.
(13) Binnig, G.; Quate, C. F.; Gerber, Ch. *Phys. Rev. Lett.* **1986**, *56*, 930.

MA971702K